Mission-Adaptive Lifting System Design using Integrated Multidisciplinary Topology Optimization

P. Ranjan * and W. Zheng †
University of Illinois at Urbana-Champaign, Urbana, Illinois 61801

K. A. James‡
University of Illinois at Urbana-Champaign, Urbana, Illinois 61801

A coupled aero-structural optimization framework for the design of a morphing wing section is proposed. A two-dimensional unstructured finite element solver and a panel-based flow solver, along with a load-transfer and mesh motion scheme constitute the fluid structure interaction system. A topology optimization sub-problem is solved for the conceptual design of an internal compliant mechanism that morphs the airfoil shape based on different c_l requirements. The proposed morphing structure is expected to achieve higher aerodynamic performance metrics when compared to a multi-point drag-optimal airfoil configuration.

I. Nomenclature

$\mathbf{A}$	=	linearized operator
$\mathbb{A}$	=	Aerodynamic residual
$\mathbf{AIC}$	=	Aerodynamic Influence Coefficient matrix
c_d	=	drag coefficient
c_l	=	lift coefficient
c_l^*	=	design lift coefficient
$\mathbf{C}$	=	gradient vector
$\mathbb{D}$	=	mesh displacement residual
$\mathbf{F}^a$	=	vector of aerodynamic forces
$\mathscr{G}$	=	coupled aeroelastic residual
$\mathbf{I}$	=	identity matrix
$\mathscr{J}$	=	objective function
$\mathbf{K}$	=	elastic stiffness matrix
m	=	mass
m_{max}	=	maximum mass
M_{pitch}	=	pitching moment
M_{max}	=	maximum pitching moment
$\mathbf{n}$	=	normal vector
p	=	PARSEC variables
$\mathbf{P}$	=	projection matrix
$\mathbb{S}$	=	elastic residual
T	=	transpose operator
$\mathbf{U}$	=	structural displacement vector
V	=	flight speed
x	=	OML displacement
w	=	flow state variable
$\mathscr{X}$	=	design variables
α	=	angle of attack
γ	=	circulation

*Graduate Research Assistant, Dept. of Aerospace Engineering, 104 S. Wright St, Student member AIAA
†Undergraduate Research Assistant, Dept. of Aerospace Engineering, 104 S. Wright St, Student member AIAA
‡Assistant Professor, Department of Aerospace Engineering,104 S. Wright St, Member AIAA

ξ = OML interface

II. Introduction

In the current day and age, aircraft design is generally governed by a multitude of factors such as aerodynamic efficiency, carbon footprint, overall cost of manufacturing and operational sustainability. Recent trends in the global aviation market suggest a shift from large four-engine multi-aisle aircraft to smaller twin engine aircraft designs. In conservative terms, the design of such aircraft systems are primarily governed by an efficient propulsion system producing minimal carbon footprint and high aspect ratio lifting systems that result in a reduction in aerodynamic drag. The design of both of these sub-systems combined contributes towards the economic success of the aircraft in a competitive global aviation market.

Design of efficient drag-optimal wing sections has been widely addressed in the open literature. Two-dimensional lifting surfaces are often designed using a numerical shape optimization routine, subject to certain design constraints such as a desired design c_l and fixed c_m. Studies such as those by Drela [1] and Samareh [2] discuss the application of medium-fidelity panel-based methods for fast and efficient airfoil shape optimization. More evolved shape optimization studies such as those by Martins *et al.* [3] and Maute *et al.* [4] discuss the application of high-fidelity flow solvers integrated with a large shape optimization framework. While these aforementioned studies emphasize high drag savings for a single design c_l, studies such as those by Nemec *et al.* [5] and Drela [1] report efficient designs as a result of multi-point considerations.

A wing section during flight is subjected to aerodynamic forces as well as corresponding structural response in the form of chord-wise bending. For a three-dimensional wing design, an additional form of structural response is the span-wise bending and torsion. Hence design of a feasible lifting surface must be approached from a multi-disciplinary standpoint in order to account for the coupled aero-structural characteristics. A decoupled design optimization routine may fail to account for coupled flight instabilities such as aeroelastic flutter and divergence. More so, the structural optimization as a second step in a sequential optimization approach does not guarantee an internal structural layout that would conform to the optimized Outer Mould Line (hereafter OML). Studies such as those by Maute *et al.* [4] , James *et al.* [6] and Martins *et al.* [3] have reported significant gains in drag savings using an integrated multidisciplinary design approach for a single flight condition.

The current study proposes an alternative design approach to a multi-point optimal airfoil configuration, using a structural compliant mechanism. A novel morphing single-element wing section is proposed wherein a compliant mechanism deflects the OML based on design c_l , producing minimum drag. The proposed morphing mechanism is used to address the multi-point design c_l requirements.

III. Numerical framework

In this study , the authors propose an integrated multidisciplinary design optimization framework for the conceptual design of the internal layout of the aero-elastic wing section. The goal of the optimization framework is to determine the structural layout that yields a deformed shape that is aerodynamically optimal in minimum drag and satisfies certain structural design constraints. At the beginning of the optimization process, only the OML of the un-deformed structure is defined.The structural and aerodynamic disciplines are thereafter optimized using a sequential Lagrangian based optimization algorithm. Fig. 1 illustrates the various sub-systems that constitute the coupled optimization framework.

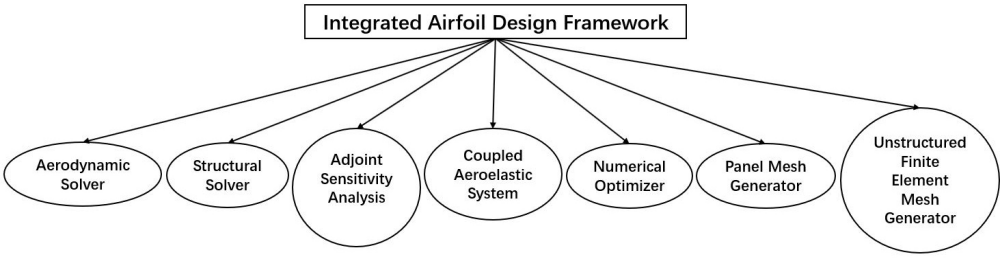

Fig. 1 Optimization framework sub-systems

The discretized form of the steady state response of the aeroelastic system is expressed as:

$$\mathscr{G} = \begin{bmatrix} \mathbb{S}(U, x_\xi, \Gamma, \alpha) \\ \mathbb{A}(U, x_\xi, \Gamma, \alpha) \\ \mathbb{D}(U, x_\xi) \end{bmatrix} \tag{1}$$

where, $\mathbb{S}$ represents the discrete structural equilibrium system of equations, expressed as:

$$\mathbb{S} : KU - F^a(x_\xi, \Gamma, \alpha) = 0 \tag{2}$$

and $\mathbb{A}$ represents the aerodynamic state equilibrium equations, expressed as:

$$\mathbb{A} : AIC.\Gamma - V = 0 \tag{3}$$

An interface boundary condition that couples the structural, aerodynamic and OML grid points is defined as:

$$\sigma.\mathbf{n} = -F^a(\Gamma, \alpha, U) \tag{4}$$

Here, σ is the structural stress tensor, $\mathbf{n}$ is the normal vector on the OML surface and F^a are the aerodynamic forces acting on the OML surface and are a function of aerodynamic state variables Γ and U.The steady state equilibrium equations for grid point displacement are expressed as:

$$\mathbb{D} : x_\xi - PU = 0 \tag{5}$$

where x_ξ are the grid locations on the OML interface ξ. $\mathbf{P}$ projects the structural displacements $\mathbf{U}$ on x_ξ [7].
Hence, the aeroelastic governing equations for each discipline of the aero-elastic system are expressed as:

$$\begin{bmatrix} \mathbb{S} \\ \mathbb{A} \\ \mathbb{D}_\xi \end{bmatrix} = \begin{bmatrix} KU - F^a \\ AIC.\Gamma - V \\ x_\xi - F^a U \end{bmatrix} = \begin{bmatrix} 0 \\ 0 \\ 0 \end{bmatrix} \tag{6}$$

If n_{struct} denotes the total structural degrees of freedom, then $\mathbf{K}$ is an $n_{struct} \times n_{struct}$ symmetric positive definite matrix. For the mesh motion solver, the degrees of freedom are $2 \times R$, where R is the total number of grid points on the OML.
The non-linear system of equations shown above has distinct numerical properties, each with different optimal solution algorithms. A partitioned procedure for solving the non-linear system of equations is proposed wherein a quasi-Newton approach is employed for building linear sub-problems and a block Gauss-Seidel scheme is used to solve these sub-problems [8].
Linearizing the non-linear system of equations about the coupled system's state variables $U, x_\xi, (w = \alpha, \Gamma)$:

$$\begin{bmatrix} \mathbb{S} \\ \mathbb{D}_\xi \\ \mathbb{A} \end{bmatrix} = \begin{bmatrix} \frac{\partial \mathbb{S}}{\partial U} & \frac{\partial \mathbb{S}}{\partial x_\xi} & \frac{\partial \mathbb{S}}{\partial w} \\ \frac{\partial \mathbb{D}}{\partial U} & \frac{\partial \mathbb{D}}{\partial x_\xi} & 0 \\ 0 & \frac{\partial \mathbb{A}}{\partial x_\xi} & \frac{\partial \mathbb{A}}{\partial w} \end{bmatrix} \begin{bmatrix} \Delta U \\ \Delta x_\xi \\ \Delta w \end{bmatrix} \tag{7}$$

The linearized operator $\mathbf{A}$ simplifies to :

$$\begin{bmatrix} \mathbf{K} & -\frac{\partial F^a}{\partial x_\xi} & -\frac{\partial F^a}{\partial w} \\ -\mathbf{P} & [0 \quad \mathbf{I}] & 0 \\ 0 & \frac{\partial \mathbb{A}}{\partial x_\xi} & \frac{\partial \mathbb{A}}{\partial w} \end{bmatrix} \tag{8}$$

The sub problems $\mathbb{S}$ and $\mathbb{A}$ will be solved using a direct method. The mesh-displacement sub-problem $\mathbb{D}$ will be solved using a Preconditioned Conjugate Gradient (PCG) algorithm.

A. Sensitivity Analysis

Sensitivity analysis of the objection function and constraints with respect to design variables drives the optimization algorithm towards an optimal solution, thus forming a critical part of the design optimization framework. Computing sensitivities or gradients of the objective generally leads to a system of linear equations with the same size of the system used in the analysis model. Thus apart from accurate calculation of the gradient vector, a fast and efficient numerical method for sensitivity analysis is necessary.

In the proposed coupled problem, the structural optimization sub-problem shall constitute of a large design space, thereby requiring an adjoint formulation. For a simple linear-elastic equilibrium formulation, the sensitivities of the strain energy with respect to material parameters are self-adjoint [9].

The proposed study employs a modified version of the adjoint formulation of Maute *et al* [8]. The derivative of the optimization criteria $\mathscr{J}$ with respect to design variables $\mathscr{X}$ is expressed as:

$$\frac{d\mathscr{J}}{d\mathscr{X}} = \frac{\partial\mathscr{J}}{\partial\mathscr{X}} + \frac{\partial\mathscr{J}^T}{\partial U}\frac{dU}{d\mathscr{X}} + \frac{\partial\mathscr{J}^T}{\partial x_\xi}\frac{dx_\xi}{d\mathscr{X}} + \frac{\partial\mathscr{J}^T}{\partial w}\frac{dw}{d\mathscr{X}} \tag{9}$$

Eq. 9 is evaluated using the adjoint approach:

$$\frac{d\mathscr{J}}{d\mathscr{X}} = \frac{\partial\mathscr{J}}{\partial\mathscr{X}} - \left(\mathbf{A}^{-T}\begin{bmatrix}\frac{\partial\mathscr{J}}{\partial U}\\ \frac{\partial\mathscr{J}}{\partial x_\xi}\\ \frac{\partial\mathscr{J}}{\partial w}\end{bmatrix}\right)^T\begin{bmatrix}\frac{\partial\mathbb{S}}{\partial\mathscr{X}}\\ \frac{\partial\mathbb{D}}{\partial\mathscr{X}}\\ \frac{\partial\mathbb{A}}{\partial\mathscr{X}}\end{bmatrix} \tag{10}$$

where, the term $\left(\cdot\right)$ represents the solution of the adjoint system.

IV. Preliminary results

A preliminary aerodynamic shape optimization study was conducted to determine the necessary OML control points and to choose an appropriate problem formulation. A multi-point design optimization study was also performed in order to compare its polar with that of the proposed morphing airfoil configuration.

The airfoil shape optimization formulation is expressed as:

$$\begin{aligned}&\min_{p_1 \ldots p_n} \; c_d\\ &\text{s.t.} \quad c_l = 0.5\end{aligned} \tag{11}$$

where, p is the vector of airfoil shape parameterization coefficients [10].

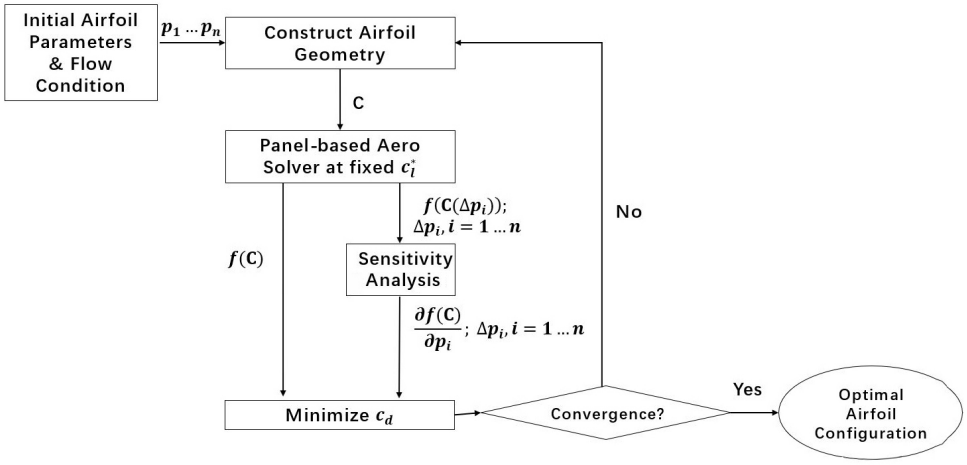

Fig. 2 Airfoil shape optimization process flow diagram

Fig. 2 represents the process flow for airfoil shape optimization. A gradient-based optimization routine is used while the sensitivities are computed using finite difference techniques. The PARSEC parameters p are used to generate the two-dimensional panel-based grid for flow solution. The number of control points are varied for three optimization cases, each producing different optimal configurations at the desired $c_l = 0.5$, subjected to a flow at Reynolds number, $\mathscr{RE}$, 500,000.

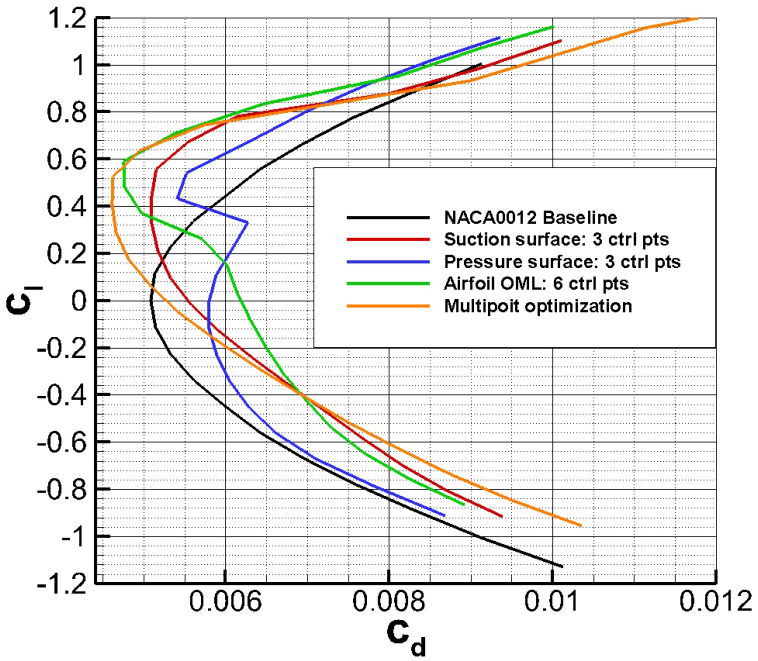

Fig. 3 Single and multi-point optimized airfoil polar

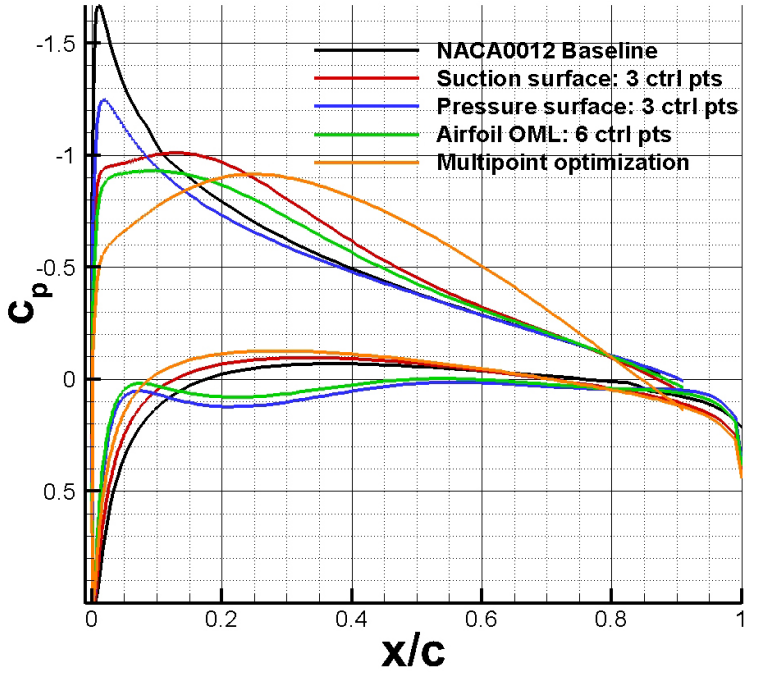

Fig. 4 C_p distribution for baseline and optimized configurations

Fig. 3 represents the performance polar for four drag-optimal airfoil configurations, plotted against the baseline NACA 0012 airfoil configuration. Favourable polar characteristics are observed for the three and six control point cases, applied to the suction side and the two sides of the OML. A cusped profile is observed for the pressure surface case which is synonymous to its corresponding airfoil profile as shown in Fig. 5 and a sudden rise in local cp, as seen in Fig. 4. The sudden increase in c_d for $c_l = 0.3$ can be attributed to local flow separation on the pressure side. The multi-point optimized configuration is observed to result in the least aerodynamic drag penalty with respect to the baseline and other configurations.

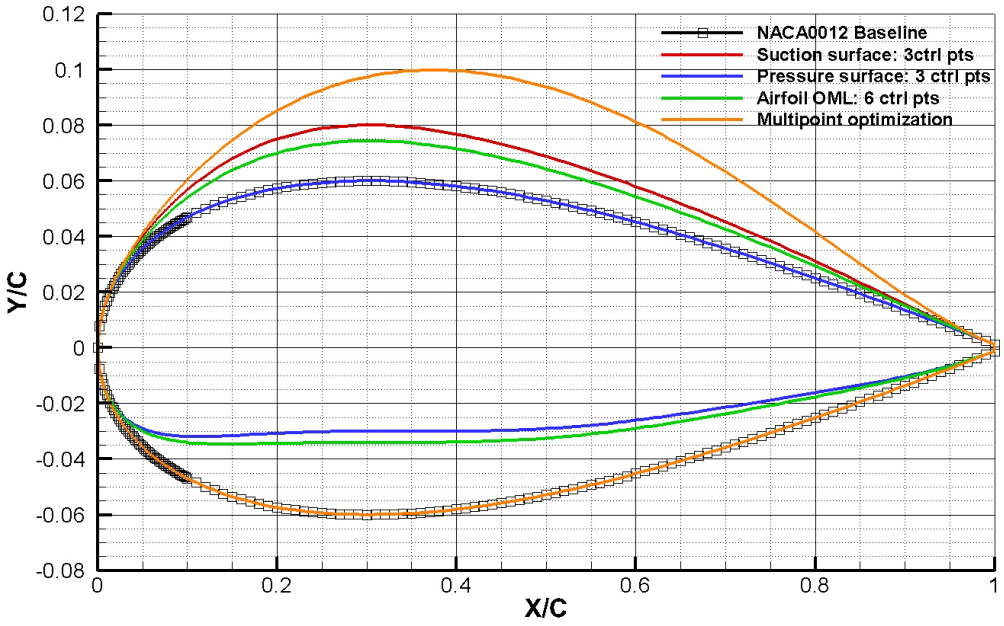

Fig. 5 Optimized airfoil configurations

V. Future work

The observations made from Figs.3 and 4 clearly illustrate the significant gains in drag reduction using a weighted multi-point design optimization framework. Such an airfoil configuration is observed to be optimal over a wide range of flight angle of attack, α, which is representative of different flight phases.

The current study proposes to address optimal airfoil design with coupled aero-structural considerations. A compliant mechanism design in proposed which morphs the airfoil OML into a drag-optimal shape for different flight regimes. The proposed multidisciplinary optimization formulation is:

$$\begin{aligned} \min_{\mathscr{X}} \quad & C_D \\ \text{s.t.} \quad & M_{pitch} - M_{max} \leq 0 \\ & c_l/c_l^* - 1 = 0 \\ & \sigma - \sigma_{yield} \leq 0 \\ & |U_{stroke}| - U_{max} \leq 0 \\ & m - m_{max} \leq 0 \end{aligned} \tag{12}$$

$$
\begin{aligned}
\min_{\mathscr{X},\alpha,\xi} \quad & C_D \\
\text{s.t.} \quad & M_{pitch} - M_{max} \leq 0 \\
& C_L = 0.5 \\
& C_{My} \leq -0.17 \\
& C - C^* \leq 0 \\
& v - v_{max} \leq 0
\end{aligned}
\tag{13}
$$

References

[1] Drela, M., "Pros and cons of airfoil optimization," *Frontiers of computational fluid dynamics*, 1998, pp. 363–381. https://doi.org/10.1142/9789812815774_0019.

[2] A, S. J., "Survey of shape parameterization techniques for high-fidelity multidisciplinary shape optimization," *AIAA journal*, Vol. 39, No. 5, 2001, pp. 877–884.

[3] Martins R A, R. J. J., Alonso J R, "High-fidelity aerostructural design optimization of a supersonic business jet," *Journal of Aircraft*, Vol. 41, No. 3, 2004, pp. 523–530.

[4] Maute K K, R. G. W., "Integrated multidisciplinary topology optimization approach to adaptive wing design," *Journal of Aircraft*, Vol. 43, No. 1, 2006, pp. 253–263.

[5] Nemec M, P. T. H., Zingg D W, "Multipoint and multi-objective aerodynamic shape optimization," *AIAA journal*, Vol. 42, No. 6, 2004, pp. 1057–1065.

[6] James K A, M. J. R., Kennedy G J, "Concurrent aerostructural topology optimization of a wing box," *Computers Structures*, Vol. 134, 2014, pp. 1–17. https://doi.org/10.1016/j.compstruc.2013.12.007.

[7] Farhat C, L. T. P., Lesoinne M, "Load and motion transfer algorithms for fluid/structure interaction problems with non-matching discrete interfaces: Momentum and energy conservation, optimal discretization and application to aeroelasticity," *Computer methods in applied mechanics and engineering*, Vol. 157, No. 1-2, 1998, pp. 95–114.

[8] Maute K, A. M., "Conceptual design of aeroelastic structures by topology optimization," *Structural and Multidisciplinary Optimization*, Vol. 27, No. 1-2, 2004, pp. 27–42.

[9] A, J. K., "Multiphase topology design with optimal material selection using an inverse p-norm function," *International Journal for Numerical Methods in Engineering*, Vol. 114, No. 9, 2018, pp. 999–1017.

[10] Ranjan P, J. K. A., "Flutter Control Using Shape and Topology Optimization," *AIAA Aviation 2019 Forum*, 2019, p. 3670.